A Role for NIMA in the Nuclear Localization of Cyclin B in *Aspergillus nidulans*

L. Wu,* S.A. Osmani,* and P.M. Mirabito‡

*Henry Hood Research Program, Weis Center for Research, Pennsylvania State University College of Medicine, Danville, Pennsylvania 17822-2617; and ‡Molecular and Cellular Biology Section, School of Biological Sciences, University of Kentucky, Lexington, Kentucky 40506-0225

Abstract. NIMA promotes entry into mitosis in late G2 by some mechanism that is after activation of the *Aspergillus nidulans* G2 cyclin-dependent kinase, $NIMX^{CDC2}/NIME^{Cyclin\ B}$. Here we present two independent lines of evidence which indicate that this mechanism involves control of $NIMX^{CDC2}/NIME^{Cyclin\ B}$ localization. First, we found that $NIME^{Cyclin\ B}$ localized to the nucleus and the nucleus-associated organelle, the spindle pole body, in a NIMA-dependent manner. Analysis of cells from asynchronous cultures, synchronous cultures, and cultures arrested in S or G2 showed that $NIME^{Cyclin\ B}$ was predominantly nuclear during interphase, with maximal nuclear accumulation in late G2. $NIMX^{CDC2}$ colocalized with $NIME^{Cyclin\ B}$ in G2 cells. Although inactivation of NIMA using either the *nimA1* or *nimA5* temperature-sensitive mutations blocked cells in G2, $NIMX^{CDC2}/NIME^{Cyclin\ B}$ localization was predominantly cytoplasmic rather than nuclear. Second, we found that *nimA* interacts genetically with *sonA*, which is a homologue of the yeast nucleocytoplasmic transporter GLE2/RAE1. Mutations in *sonA* were identified as allele-specific suppressors of *nimA1*. The *sonA1* suppressor alleviated the nuclear division and $NIME^{Cyclin\ B}$ localization defects of *nimA1* cells without markedly increasing $NIMX^{CDC2}$ or NIMA kinase activity. These results indicate that NIMA promotes the nuclear localization of the $NIMX^{CDC2}/NIME^{Cyclin\ B}$ complex, by a process involving SONA. This mechanism may be involved in coordinating the functions of $NIMX^{CDC2}$ and NIMA in the regulation of mitosis.

Entry into mitosis in *Aspergillus nidulans* is regulated by the coordinate function of two serine/threonine protein kinases, $NIMX^{CDC2}$ and NIMA. $NIMX^{CDC2}$ is an essential histone H1 kinase that is structurally and functionally homologous to fission yeast $p34^{cdc2}$ (Osmani et al., 1994). NIMA is a β-casein kinase and is structurally distinct from $p34^{cdc2}$, containing an amino-terminal catalytic domain and a carboxyl-terminal regulatory domain (Osmani et al., 1988*b*; Lu et al., 1993; Pu and Osmani, 1995; Pu et al., 1995). Failure to properly activate either of these kinases in G2 prevents the initiation of mitosis, and the combined action of both kinases is critical for coordinating changes in chromosome, microtubule, and nuclear membrane structure during mitosis. For example, mutations preventing the activation of $NIMX^{CDC2}$ in G2 normally arrests cells in late G2 (Osmani et al., 1991*a*; 1994). Although overexpression of NIMA can overcome this interphase arrest, the ensuing mitosis is disorganized such that chromosome condensation occurs but normal spindle assembly does not (O'Connell et al., 1994; Pu and Osmani, 1995). Likewise, *nimA* mutations normally arrest cells in late G2 (Osmani et al., 1987; 1991*a*). Although a $bimE^{APC1}$ checkpoint mutation can overcome this G2 arrest, the ensuing mitosis is disorganized and includes aberrant spindle, chromatin, and nuclear membrane structure (Osmani et al., 1988*a*; 1991*b*).

To ensure the coordinated function of $NIMX^{CDC2}$ and NIMA, each kinase must somehow be sensitive to the function of the other. Phosphorylation of NIMA by $NIMX^{CDC2}$ is likely to be involved in making NIMA function sensitive to $NIMX^{CDC2}$ at the G2 to M transition (Ye et al., 1995). Before activation of $NIMX^{CDC2}$ in late G2, NIMA is hypophosphorylated and active as a β-casein kinase. Upon activation of $NIMX^{CDC2}$, NIMA is converted to a hyperphosphorylated, slightly more active form that reacts well with the antiphosphoprotein antibody, MPM2. The finding that $NIMX^{CDC2}$ is necessary for NIMA hyperphosphorylation and MPM2 reactivity in vivo, and is sufficient for NIMA hyperphosphorylation and MPM2 reactivity in vitro, is consistent with a direct role for $NIMX^{CDC2}$ in NIMA hyperphosphorylation (Ye et al., 1995).

Address all correspondence to P.M. Mirabito, Molecular and Cellular Biology Section, School of Biological Sciences, University of Kentucky, Lexington, KY 40506-0225. Tel.: (606) 257-7642. Fax: (606) 257-1717. E-mail: pmmira000@pop.uky.edu

The role of NIMA hyperphosphorylation in NIMA's function as a mitotic regulator remains to be determined. Hyperphosphorylated NIMA is detectable coincident with the initiation of mitosis in synchronous cultures, consistent with hyperphosphorylation playing a positive role in NIMA's function as a mitotic inducer (Ye et al., 1995). This stimulatory effect could be at the level of NIMA activity, since hyperphosphorylation causes a twofold increase in NIMA's β-casein kinase activity. Hyperphosphorylation could also regulate NIMA function at other levels, for example, by regulating NIMA localization or NIMA proteolysis. The identification of several consensus CDC2 phosphorylation sites in NIMA's carboxyl terminus (Osmani et al., 1988*b*; Fry and Nigg, 1995) and the requirement of the carboxyl terminus for NIMA proteolysis (O'Connell et al., 1994; Pu and Osmani, 1995) is suggestive of hyperphosphorylation playing a role in regulating NIMA turnover.

If there is a mechanism making $NIMX^{CDC2}$ function sensitive to NIMA activity, it does not involve regulation of $NIMX^{CDC2}$ activation (Osmani et al., 1991*a*). Like most eukaryotic cells (Nurse, 1990), activation of CDC2 during G2 in *Aspergillus* is mediated by its binding to the Cyclin B homologue, $NIME^{Cyclin\ B}$, which is the principle B-type cyclin associated with activated $NIMX^{CDC2}$ during G2 (Bergen et al., 1984; Osmani et al., 1994; James et al., 1995). $NIMX^{CDC2}/NIME^{Cyclin\ B}$ is activated by dephosphorylation of tyrosine residue 15 on $NIMX^{CDC2}$ (O'Connell et al., 1992; Osmani et al., 1994). Tyrosine phosphorylation of $NIMX^{CDC2}$ requires the function of the $p107^{wee1}$ homologue, $ANKA^{WEE1}$, (Ye et al., 1996), and tyrosine dephosphorylation requires the function of the $p80^{cdc25}$ homologue, $NIMT^{CDC25}$ (O'Connell et al., 1992). *nimA* mutations cause a specific cell cycle arrest in G2 very close to the $nimT^{cdc25}$ mutant arrest point, yet they do not prevent formation of a $NIMX^{CDC2}/NIME^{Cyclin\ B}$ complex, dephosphorylation of $NIMX^{CDC2}$ on tyrosine 15, or activation of the $NIMX^{CDC2}/NIME^{Cyclin\ B}$ complex as a histone H1 kinase (Osmani et al., 1991*a*; Pu et al., 1995). Furthermore, the *nimA5* mutation prevents mitosis even in strains expressing a mutant form of $NIMX^{CDC2}$ which cannot be phosphorylated on threonine 14 or tyrosine 15 (Ye et al., 1996). Thus, loss of NIMA function prevents mitosis by some mechanism other than regulation of the activity of $NIMX^{CDC2}/NIME^{Cyclin\ B}$.

One way in which $NIMX^{CDC2}$ function could be affected by NIMA would be if NIMA function was required for proper localization of activated $NIMX^{CDC2}$. It is known that CDC2/cyclin localization is regulated for certain cyclin-dependent kinase complexes (for example see Pines and Hunter, 1991; Gallant and Nigg, 1992; Ookata et al., 1992; Maridor et al., 1993; Ookata et al., 1995). Here we present evidence from two independent lines of investigation supporting a role for NIMA in the subcellular localization of $NIMX^{CDC2}/NIME^{Cyclin\ B}$. First, using indirect immunofluorescence analysis of fixed cells, we found that $NIMX^{CDC2}$ and $NIME^{Cyclin\ B}$ localized to the nucleus and the nuclear-associated organelle, the spindle pole body (SPB)[1], in a NIMA-dependent manner. Second, using suppressor analysis, we found that mutations in a homologue of the nucleocytoplasmic transporter GLE2/RAE1 (Brown et al., 1995; Murphy et al., 1996) act as allele-specific suppressors of the *nimA1* mutation. Together, these results suggest a role for NIMA in the nuclear localization of the $NIMX^{CDC2}/NIME^{Cyclin\ B}$ and they provide evidence for a mechanism by which $NIMX^{CDC2}/NIME^{Cyclin\ B}$ function is made sensitive to NIMA to coordinate the action of these two mitotic promoting kinases.

Materials and Methods

Strains, Microbiological Techniques, and Genetic Analyses

Aspergillus strains used in this study are listed in Table I. Standard conditions were used for *Aspergillus* propagation (Morris, 1976; Kafer, 1977), genetics (Pontecorvo et al., 1953), and transformation (Osmani et al., 1987; Gems et al., 1991, 1994). The conditions and procedures used to grow *A. nidulans* cultures and isolate protein extracts were as described previously (Ye et al., 1995) except where noted in the text. For cytological analyses, *A. nidulans* cells were grown in liquid YG (Morris, 1976) on coverslips as previously described (Mirabito and Morris, 1993).

Fluorescence Microscopy

Cells were fixed and stained with 4′,6-diamidino-2-phenylindole (DAPI) to visualize nuclei as previously described (Osmani et al., 1987). Cells were fixed and prepared for indirect immunofluorescence microscopy as previously described (Mirabito and Morris, 1993) with the following exceptions. Cell walls were removed using 40 mg/ml novozyme 234 (NOVO 234) (InterSpex Products, San Mateo, CA), 80 mg/ml Driselase (Interspex Products, Foster City, CA), 1 mM diisopropyl fluorophosphate (DIFP) (Sigma Chemical Co., St. Louis, MO), 2 μg/ml leupeptin, and 40 mg/ml Aprotinin (Sigma Chemical Co.). Lipids were extracted using −20°C methanol for 8 min followed by −20°C acetone for 30 s. Lipid extraction using room temperature methanol or 1% NP-40 yielded similar results. Coverslips were mounted on mounting medium (90% glycerol in TBS containing 1 mg/ml *p*-phenylenediamine).

Primary Abs used were 12CA5 (Berkeley Antibody Co., Richmond, CA) at 10 mg/ml; rabbit anti-$NIME^{Cyclin\ B}$ serum E8 (Osmani et al., 1994) at 1:1,000; preimmune rabbit serum E8 at 1:1,000; rabbit anti-$NIMX^{CDC2}$ serum E77 (Osmani et al., 1994) at 1:1,000; preimmune rabbit serum E77 at 1:1,000; MPM2 (gift of J. Kuang, M.D. Anderson Cancer Center, Houston, TX) at 1:1,000; affinity-purified rabbit anti-γ-tubulin (gift of B. Oakley, Ohio State University, Columbus, OH) at 1:100; anti-histone H1 mouse mAb (gift of A. Epstein, University of Southern California, School of Medicine, Los Angeles, CA) at 1:1,000; and DM1A (Sigma Chemical Co.) at 1:100. Secondary Abs (Jackson ImmunoResearch Laboratories, Inc., West Grove, PA) were CY3-labeled, goat anti–mouse IgG at 1:500, dichlorotriazinylamino fluorescein (DTAF)-labeled, goat anti–mouse IgG at 1:250, CY3-labeled, goat anti–rabbit IgG at 1:500, and DTAF-labeled, goat anti–rabbit IgG at 1:250. Photomicrographs of cells stained with 12CA5 within each figure were produced using identical conditions of fixation, staining, exposure, and enlargement.

For colocalization of $NIME^{Cyclin\ B}$ and SPB or nuclear antigens, some experiments involved double staining using two mouse mAbs (12CA5 and anti-histone H1 or 12CA5 and MPM2). For these experiments, fixed cells were incubated first in 12CA5 and then in a conjugated, anti-mouse secondary antibody, and then in 20 mg/ml of unconjugated, anti-mouse Fab fragments (Jackson ImmunoResearch Laboratories, Inc.) before incubation in the second mouse mAb. This treatment effectively blocked all the anti-mouse IgG sites on the 12CA5 mAb: no further binding to 12CA5 was detectable in control experiments. Colocalization of $NIME^{Cyclin\ B}$ and SPBs was confirmed using 12CA5 and the affinity-purified, rabbit anti–γ-tubulin Ab.

Photomicrographs were captured using either a Photometrics charge-coupled device (CCD) camera (model Sensys; Tucson, AZ) and manipulated using Phase 3 Imaging Systems software (Sterling Heights, MI) (see Fig. 8) or a Diagnostics Instruments Inc., (Media Cybernetics, Silver Spring, MD) CCD camera and then manipulated using Adobe Photoshop 4.0 (Adobe Systems, Inc., San Jose, CA).

1. *Abbreviations used in this paper*: CCD, charge-coupled device; cs, cold sensitive; DAPI, 4′,6-diamidino-2-phenylindole; HA, hemagglutinin; ORF, open reading frame; SPB, spindle pole body; ts, temperature sensitive.

Culture Conditions for NIME Localization Studies

For analysis of NIME$^{Cyclin\ B}$ and NIMX^{CDC2} localization in exponentially growing asynchronous cultures, cells were incubated in YG on coverslips at 32°C for 8–12 h. For analysis of NIME localization in cells arrested in S phase, cells were incubated in YG at 32°C for 6 h and then hydroxyurea was added at 50 mM and incubation was continued for an additional 3 h at 32°C. For analysis of NIME$^{Cyclin\ B}$ and NIMX^{CDC2}, localization in cultures shifted to restrictive temperature, cells were incubated in YG liquid at permissive temperature until they contained an average of 2–4 nuclei, and then the cultures were placed in a 44°C incubator for up to 6 h. To generate synchronous cultures, *nimT*^{cdc25} or *nimA* mutants were germinated for 2 h at 32°C, shifted to 44°C for 5 h to arrest cells in G2 of their first cell cycle. The cells were shifted back to either 32°C or room temperature by replacing the medium. Samples were taken before the shift and at the times after the shift as indicated in the legends to Figs. 3 and 5.

Isolation and Characterization of Strains Carrying the sonA1 Suppressor Mutation

Spores of the temperature-sensitive (ts) *nimA1* strain, LPW2, were mutagenized with 4-nitroquinoline-1-oxide as described (Harris et al., 1994) to achieve a kill rate of 80–95%. The survivors were plated on MAG medium (2% malt extract, 0.2% peptone, 1% dextrose, 2% agar) and incubated at 42°C for 3 d. Revertants were isolated at a frequency of 1,487 revertants out of 4×10^8 survivors plated. Revertants were patched to MAG plates and incubated at 20°C for 8 d to screen for cold sensitivity. Out of 1,487 revertants, 35 were cold sensitive. To screen for extragenic suppressors, each cold-sensitive (cs) revertant was crossed to A612 and random meiotic progeny were selected and scored for the ts and cs phenotypes. Three out of the 35 cs revertants yielded both ts and cs meiotic progeny and demonstrated linkage of the cs and *nimA1* suppression phenotypes. This indicated that these revertants contained the *nimA1* mutation and a cs, extragenic suppressor of *nimA1*. Complementation analysis in diploids and genetic crosses indicated that three alleles of a single suppressor gene had been isolated. We named this gene *sonA* for suppressor of *nimA1*. Dominance/recessiveness was determined by generating diploids between each revertant and strain A154. The suppressor mutation was assigned to chromosome VIII using standard parasexual analysis (Pontecorvo et al., 1953).

Cloning and Characterization of sonA

Standard procedures were used for DNA preparation and manipulation (Sambrook et al., 1989). Wild-type *sonA* was cloned by complementation of the cs phenotype of LPW16 using a chromosome VIII–specific cosmid library (Brody et al., 1991) and the autonomously replicating plasmid pAR1-*pyr4* (Verdoes et al., 1994) using standard procedures (Gems et al., 1991, 1994). Individual cosmids capable of complementing *sonA1* were identified by sib selection. A common 2.6-kb HindIII fragment was the smallest restriction fragment from these cosmids capable of complementing *sonA1* in trans. This fragment was sequenced using an Applied Biosystems DNA sequencer (model 373A; Foster City, CA) using procedures recommended by the manufacturer. Open reading frame (ORF) identification and sequence alignments were preformed using the Applied Biosystems Sequence Analysis Program. Database searches were preformed using BLAST (Altschul et al., 1990).

The *sonA* cDNA was isolated by PCR of *A. nidulans* total cDNA using Vent polymerase (New England BioLabs, Inc., Beverly, MA). The isolated cDNA covers the entire ORF of SONA, starting at 90 bp upstream from the start codon and ending 32 bp downstream from the stop codon. The sequence for the forward primer was 5′-GCTCTTGATACCCGTCTCTC-3′and for the reverse primer was 5′-CGAATGATGACTAGCCTGGAG-3′.

To determine whether the cloned gene was *sonA* or a suppressor of *sonA1*, we integrated the cloned gene at its homologous locus in the *sonA1* strain, LPW16, using a two-step gene replacement procedure (O'Connell et al., 1992). In the first step, plasmid pRSW2, containing the *sonA1* complementing gene and the *A. nidulans pyrG* gene, was used to transform LPW16, converting LPW16 from cs to wild-type growth at 20°C. Plasmid pRSW2 was constructed by inserting an EcoRI/BamHI genomic *sonA* fragment (containing the wild-type *sonA* gene from 284 bp upstream of the ATG to 140 bp downstream from the stop codon) into pRG3 (Waring et al., 1989). In the second step, a transformant was plated on medium containing uracil and 5-fluoroorotic acid to select for plasmid loss. Both cs and wild-type isolates were obtained as 5-fluoroorotic acid–resistant sectors and plasmid loss was confirmed by Southern blot analysis. Wild-type isolates were confirmed to have lost the *sonA1* mutation by standard genetic analysis.

A strain expressing endogenous SONA1 and a recombinant SONA fused to two tandem copies of the hemagglutinin (HA) epitope at its carboxyl terminus (SONA-HA) was created by transforming pMTW2 into LPW16. Plasmid pMTW2, containing *sonA* fused to two tandem HA epitopes was constructed as follows: a *sonA* PCR fragment containing 284 bps upstream from the start codon and 140 bps downstream from the stop codon was inserted into pRG3 as a BamHI/EcoRI fragment. A sequence encoding two tandem HA epitopes (5′-TACCCATACGATGTTCCTGACTATGCGGGCTATCCCTATGACGTCCCGGACTATGCGGA-3′) was inserted into the *sonA* gene immediately before the stop codon by site-directed mutagenesis using the Quick Change™ mutagenesis kit (Strategene, La Jolla, CA). Expression of SONA-HA complemented the cs phenotype of *sonA1* and was verified by Western blot analysis using 12CA5.

Analysis of Protein Kinase Levels

To prepare cultures for protein kinase studies, 10^6 spores/ml were inoculated into flasks containing YG liquid medium and then were shaken at 250 rpm at 32°C for 10 h. For analysis of asynchronous cultures, samples were collected and processed after 10 h at 32°C. For analysis of cultures shifted to restrictive temperature, cultures were brought to 42°C and sampled at the times indicated in Fig. 10. For analysis of cultures shifted back to permissive temperature, 3h, 42°C cultures were brought back to 32°C and sampled at the times indicated in Fig. 10. Procedures for sampling, protein isolation, and protein kinase assays were as previously described (Osmani et al., 1991*a*; Ye et al., 1995).

Results

NIME$^{Cyclin\ B}$ Localized Predominantly to the Nucleus

To determine the subcellular localization of NIME$^{Cyclin\ B}$, we have created a number of *A. nidulans* strains (Table I) in which the wild-type NIME$^{Cyclin\ B}$ gene (*nimE*$^{Cyclin\ B}$) has been replaced with an HA-tagged version of *nimE*$^{Cyclin\ B}$ (*HA-nimE*$^{Cyclin\ B}$) (Osmani et al., 1994). These strains are phenotypically identical to coisogenic strains containing the untagged version (data not shown), and we can detect HA-NIME$^{Cyclin\ B}$ using the mAb, 12CA5. HA-NIME$^{Cyclin\ B}$ localized predominantly to the nucleus in rapidly growing wild-type cells (Fig. 1, *top row*). Approximately half of the cells in exponentially growing asynchronous cultures showed detectable nuclear HA-NIME$^{Cyclin\ B}$ staining, whereas essentially every cell showed nuclear staining with anti-histone H1 mAb. The percentage of cells in asynchronous cultures which exhibited nuclear HA-NIME$^{Cyclin\ B}$ staining was consistent in multiple experiments. The nuclear NIME$^{Cyclin\ B}$ staining was punctate and included chromatin, the nucleolus, and the SPB, as judged by staining with 12CA5, DAPI, and either anti–γ-tubulin Ab or MPM2 (Figs. 1 and 2; data not shown). Faint staining of the cytoplasm in cells with bright nuclear staining was also detected. Double staining with 12CA5 and the anti-tubulin Ab, DM1A, showed that all of the cells with nuclear HA-NIME$^{Cyclin\ B}$ contained cytoplasmic microtubules and that cells with mitotic spindles lacked nuclear-specific HA-NIME$^{Cyclin\ B}$ staining (Fig. 1, *bottom two rows*).

The lack of nuclear NIME$^{Cyclin\ B}$ staining in all cells of an asynchronous culture suggested that nuclear NIME$^{Cyclin\ B}$ localization might be cell cycle stage-specific. To preliminarily investigate this possibility, we localized HA-NIME$^{Cyclin\ B}$ in cells blocked in S phase with hydroxyurea or in late G2

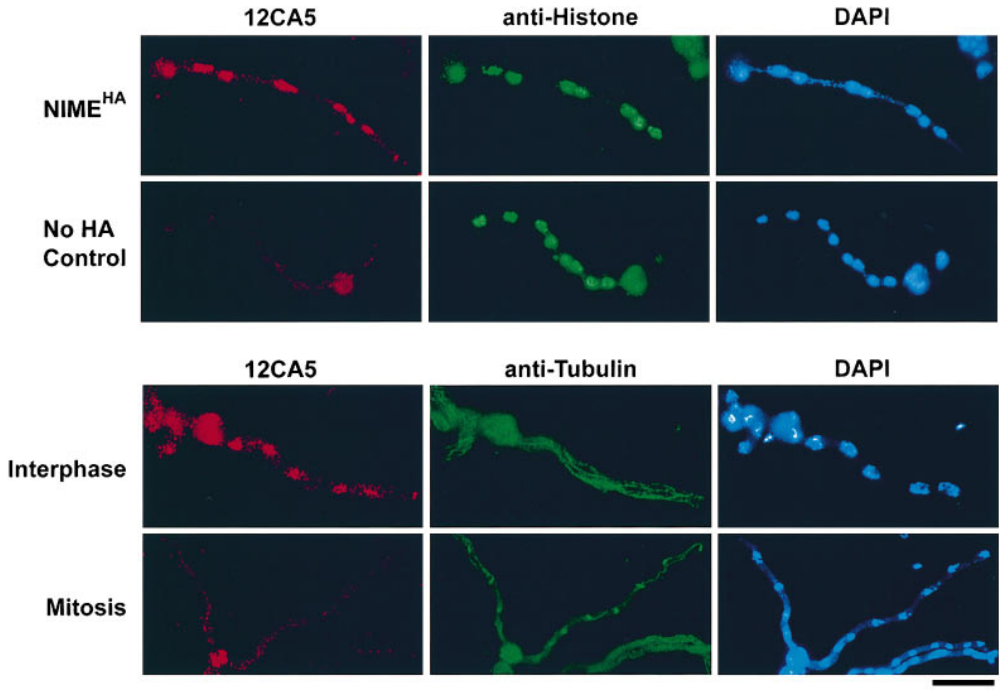

Figure 1. In situ localization of NIME$^{Cyclin\ B}$ in wild-type cells. Cells of PMC654-4, the strain expressing HA-NIME$^{Cyclin\ B}$ (*first*, *third*, and *fourth rows*) and R153, the no-HA control strain (*second row*), were cultured, fixed, and then prepared for immunocytology as described in Materials and Methods. Each row shows three images of the same cell. The images corresponding to Ab or DAPI staining are labeled above the panels. Note on cell morphology: *A. nidulans* is a filamentous fungus that undergoes polar growth and nuclear division without cytokinesis during much of its life cycle. Each elongated, multinucleate cell, or hypha, shown here is the result of the polarized growth and multiple, synchronous nuclear divisions of a uninucleate spore. Hyphal compartments are formed by growth and septation, with all nuclei within one compartment being synchronous. The large bulge at one end of each cell is the spore from which the cell originated. Bar, 10 μm.

with a ts mutation in *nimT*^{cdc25}. Both treatments gave essentially the same result: the frequency of nuclear HA-NIME$^{Cyclin\ B}$ staining increased to essentially 100% when cells were blocked in S or G2. Fig. 2 shows examples of the results for cells blocked in G2 by the *nimT*^{cdc25} mutation. As cells accumulated at the *nimT*^{cdc25} G2 arrest point, nuclear staining became increasingly brighter. The 12CA5 staining result was confirmed by double staining with 12CA5 and polyclonal rabbit anti-NIME$^{Cyclin\ B}$ serum (Osmani et al., 1994). Both Abs stained nuclei, including chromatin, the nucleolus, and SPB-like dots (Fig. 2, *top row*). To determine if NIMX^{CDC2} colocalized with NIME$^{Cyclin\ B}$, we performed double labeling experiments using 12CA5 and polyclonal rabbit anti-NIMX^{CDC2} specific antisera (Osmani et al., 1994). NIME$^{Cyclin\ B}$ and NIMX^{CDC2} colocalized on nuclei (Fig. 2, *middle row*). Preimmune serum controls for the anti-NIME and anti-NIMX antisera showed no nuclear specific staining (data not shown). Nuclear staining was also obtained using rabbit anti-NIME$^{Cyclin\ B}$ and anti-NIMX^{CDC2} sera on a *nimT*^{cdc25} mutant strain which expressed only untagged NIME$^{Cyclin\ B}$ (data not shown).

To determine if the nuclear-associated dots were indeed SPBs, we performed double labeling experiments using polyclonal rabbit anti-NIME$^{Cyclin\ B}$ serum and the mouse mAb, MPM2, which stains the SPB of G2 cells (Martin et al., 1997). Anti-NIME$^{Cyclin\ B}$ and MPM2 staining colocalized on SPBs and the nucleolus in *nimT*^{cdc25}-arrested cells (Fig. 2, bottom row). Double labeling with 12CA5 and anti–γ-tubulin, or with anti-NIMX^{CDC2} sera and MPM2 gave similar results (data not shown).

To further characterize the cell cycle dependency of NIME$^{Cyclin\ B}$ localization, we determined the localization of HA-NIME$^{Cyclin\ B}$ in cycling cells from synchronous cultures. We generated synchronous cultures by blocking cells in late G2 using a *nimT*^{cdc25} mutation and then releasing the cell cycle arrest. Immediately before release from the G2 arrest, 100% of the cells showed nuclear HA-NIME$^{Cyclin\ B}$ staining (Fig. 3). Within 10 min after release from the G2 arrest, 90% of the cells entered mitosis and showed no nuclear HA-NIME$^{Cyclin\ B}$ staining, whereas the cells in the same sample that had not yet entered mitosis continued to show nuclear HA-NIME$^{Cyclin\ B}$ staining (Fig. 3 *B*). By 20 min after release, all the cells had finished mitosis (Fig. 3 *A*) and no cells (out of more than 300 examined) exhibited nuclear HA-NIME$^{Cyclin\ B}$ staining. Cells with nuclear HA-NIME$^{Cyclin\ B}$ began to accumulate 80 min after the release and almost all of the cells exhibited nuclear HA-NIME$^{Cyclin\ B}$ staining (Fig. 3, *A* and *B*) just before initiation of the second mitosis. As with the first mitosis, nuclear HA-NIME$^{Cyclin\ B}$ staining was lost coincident with the initiation of mitosis. Out of more than a thousand mitotic cells examined, only two showed very faint nuclear NIME^{HA} staining. Essentially all cells showed SPB staining at the initial G2 arrest point and in G2 just before the second division (data not shown). SPB staining was not distinguishable from chromatin or nucleolar staining in cells at other time points.

NIME$^{Cyclin\ B}$ Localizes Predominantly to the Cytoplasm in nimA Mutants

To investigate the possibility that NIMA is involved in NIMX^{CDC2}/NIME$^{Cyclin\ B}$ localization, we constructed strains expressing HA-NIME$^{Cyclin\ B}$ and carrying the ts *nimA5* or *nimA1* mutations. We determined the localization of HA-NIME$^{Cyclin\ B}$ in these strains at restrictive and permissive temperature. At permissive temperature,

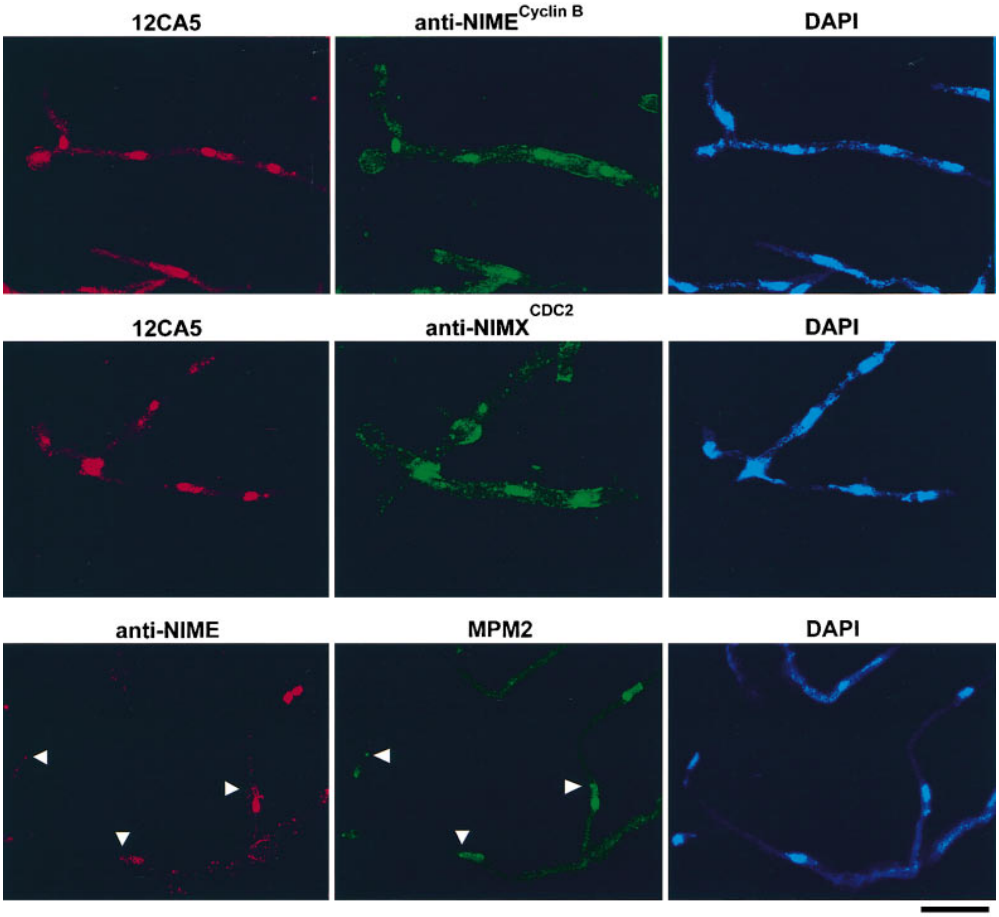

Figure 2. Localization of NIME$^{Cyclin\ B}$ and NIMX^{CDC2} on nuclei and SPBs in cells arrested in late G2 by a *nimT*^{cdc25} mutation. SFC4-21 cells were cultured, fixed, and then prepared for immunocytology as described in Materials and Methods. The cells contained 4–8 elongated, well separated nuclei characteristic of cells arrested in late G2 by a *nimT*^{cdc25} mutation (James et al., 1995). The images corresponding to Ab or DAPI staining are labeled above each image. Arrows point to coincident staining of SPBs by anti-NIME$^{Cyclin\ B}$ and MPM2. Bar, 10 μm.

about half the cells from asynchronous cultures of *nimA5* or *nimA1* mutants showed nuclear HA-NIME$^{Cyclin\ B}$ localization (data not shown). In contrast, after the shift to restrictive temperature, the *nimA5* and *nimA1* cells showed little nuclear-specific HA-NIME$^{Cyclin\ B}$ staining (Fig. 4). Instead of being concentrated at nuclei, HA-NIME$^{Cyclin\ B}$ staining was diffuse throughout the cell. Although *nimA* and *nimT*^{cdc25} mutants arrest at essentially the same point in late G2, their NIME$^{Cyclin\ B}$ staining patterns are dramatically different (Fig. 4, compare *top row* with *second* and *third rows*). Antibody access to the nuclei of these cells was confirmed by staining with MPM2 (Fig. 4, *middle column*) and anti-histone H1 antibodies (data not shown).

Table I. A. nidulans Strains Used in This Study

Strain	Genotype	Reference
A154	*adE20; biA1; wA2, cnxE16; sC12: methG11; nicA2; lacA1; choA1; chaA1*	FGSC*
A612	*acrA1; riboB2; chaA1*	FGSC
GR5	*wA2; pryG89; pyroA4*	FGSC
LPW2	*riboA1; wA2; nimA1; nicA2*	This study
LPW16	*pyrG89; wA2; sonA1*	This study
LPW29	*pyrG89, riboB2; wA2; nimA1; sonA1*	This study
LPW42	*LPW16 transformed with pMTW2*	This study
PMC645-4	*HA-nimE, wA2, cnxE16; nicA2*	This study
PMC654-19	*HA-nimE; cnxE16; nimA5; nicA2; chaA1*	This study
R153	*wA3; pyroA4*	FGSC
SFC4-21	*pabaA1, yA2; HA-nimE, nimT23; nicA2; choA1*	This study
SFC403-19	*riboA1, pabaA1; HA-nimE; nimA1; methG11; choA1; chaA1*	This study
SFC444-1	*pabaA1; HA-nimE; nimA1; nicA2; choA1; sonA1*	This study
SFC612-5	*riboA1; HA-nimE; nimA5; sonA1*	This study

*FGSC, Fungal Genetics Stock Center, Department of Microbiology, University of Kansas Medical Center, Kansas City, Kansas 66160-7420.

It was possible that the above results were caused by masking of the single HA epitope of HA-NIME$^{Cyclin\ B}$ in *nimA* mutants. To address this possibility, we stained *nimA5* cells cultured at restrictive temperature with polyclonal rabbit anti-NIME$^{Cyclin\ B}$ and anti-NIMX^{CDC2} sera. As with 12CA5 staining, anti-NIME$^{Cyclin\ B}$ staining was diffuse throughout the cells of *nimA* mutants (Fig. 4, *second row*). Similar results were obtained with anti-NIMX^{CDC2} serum (Fig. 4, *bottom row*).

Like the *nimT*^{cdc25} mutation, the *nimA5* mutation is readily reversible. A few minutes after return to permissive temperature, *nimA5* mutants leave G2 and enter mitosis synchronously (Oakley and Morris, 1983; Osmani et al., 1991*a*). If nuclear NIME$^{Cyclin\ B}$ localization is important for mitotic initiation, then one would predict that NIME$^{Cyclin\ B}$ would reaccumulate on nuclei of *nimA* mutants as cells approach mitosis after return to permissive temperature. To test this, we compared the nuclear HA-NIME$^{Cyclin\ B}$ staining profiles of a *nimA5* and a *nimT*^{cdc25} mutant at their arrest point in G2 and after release from the G2 arrest into room temperature medium. Release from the G2 arrest under these conditions is relatively slow, allowing for ex-

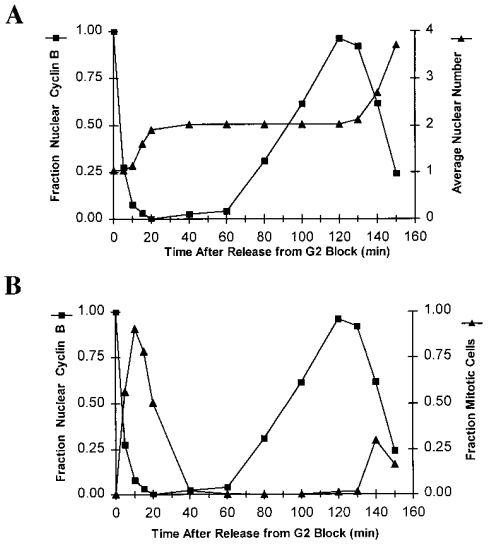

Figure 3. Kinetic analysis of NIME$^{Cyclin\ B}$ localization in cells from a synchronized culture. Cells of the *nimT^{cdc25}* mutant, SFC4-21, were cultured, fixed, and then prepared for immunocytology as described in Materials and Methods. The cells were stained for HA-NIME$^{Cyclin\ B}$, α-tubulin, and DAPI. *A* and *B* present data from the same samples plotted to show the fraction of cells with nuclear NIME^{HA} (■) relative to nuclear division (▲) in *A* or relative to spindle formation (▲) in *B*. Each value was determined by counting more than 300 cells.

amination of cells as they progress from very late G2 into early mitosis. As above, the percentage of *nimT^{cdc25}* cells with nuclear HA-NIME$^{Cyclin\ B}$ decreased after release from the G2 block (Fig. 5 *A*). In contrast, the percentage of *nimA5* cells showing nuclear HA-NIME$^{Cyclin\ B}$ staining increased after release from the block, with 40% of the cells having nuclear HA-NIME$^{Cyclin\ B}$ staining 2 min after the release (Fig 5 *B*). Under these conditions, reduced but detectable nuclear HA-NIME$^{Cyclin\ B}$ staining remained in some early mitotic cells with very short spindles, although the majority of mitotic cells and all mitotic cells at metaphase or beyond were negative for nuclear HA-NIME$^{Cyclin\ B}$. All of the *nimA5* cells eventually progressed through mitosis and showed no nuclear nimE$^{Cyclin\ B}$ staining (data not shown). Based on our observations, it is likely that most if not all *nimA5* cells accumulated nuclear HA-NIME$^{Cyclin\ B}$ after return to permissive temperature. The slow, somewhat asynchronous release under these conditions coupled with the loss of nuclear HA-NIME$^{Cyclin\ B}$ staining early in mitosis probably accounts for the shallow slope of nuclear HA-NIME$^{Cyclin\ B}$ curve in Fig. 5 *B*. We did not observe obvious SPB-like HA-NIME$^{Cyclin\ B}$ staining in *nimA5* cells after return to permissive temperature.

nimA Interacts Genetically with sonA, a Gene Related to the Nucleocytoplasmic Transporters GLE2 and RAE1

As part of a search for *nimA*-interacting genes, we have attempted to identify extragenic suppressors of *nimA* mutations by isolating induced revertants of the *nimA1* heat-sensitive (ts) mutation (refer to Materials and Methods). *nimA1* is a tight ts mutation, with colony formation severely inhibited at 42°C, a temperature at which wild-type strains grow well (Fig. 6). We isolated a number of revertants which were simultaneously converted from heat sensitive (ts) to cs, being able to form colonies normally at 42° but not at 20°C (see LPW29 in Fig. 6). For three of these revertants, suppression of *nimA1* was unlinked to *nimA* and tightly linked to the cs phenotype, demonstrating that the original revertants contained a cs, extragenic suppressor of *nimA1* (data not shown). These suppressor mutations also conferred a cs phenotype in a *nimA1* background (see LPW16 in Fig. 6). All three cs mutations were recessive and in the same complementation group (data not shown), which we designated *sonA* for suppressor of *nimA1*. One of these mutations, *sonA1*, was chosen for further study.

We cloned the wild-type *sonA* gene by complementation of the cs defect of a *sonA1* mutant (refer to Materials and Methods). A cosmid clone capable of complementing *sonA1* was recovered and the complementing sequence was localized to a 2.6-kb genomic fragment. A cDNA clone, generated by PCR, was also sufficient for complementation of *sonA1*. Sequence of the genomic and cDNA clones indicated that the complementing fragment encoded a 1.2-kb ORF interrupted by a single, 65-bp intron (Fig. 7 *B*). The cloned gene was *sonA* and not a suppressor of *sonA1* because it was tightly linked to *sonA* (refer to Materials and Methods) and because the sequence of this gene in the *sonA1* strain contained a single C to G mutation resulting in a *P* to R change at amino acid residue 205 in the ORF (Fig. 7 *A*).

Conceptual translation of the *sonA* ORF predicts that the *sonA* polypeptide (SONA) contains 362 amino acid residues corresponding to a mol wt of ~39.5 kD. Sequence database searches revealed that SONA is highly similar to *Schizosaccharomyces pombe* RAE1 (Brown et al., 1995) and *Saccharomyces cerevisiae* GLE2 (Murphy et al., 1996). SONA is 84.3% similar (58.8% identical) to RAE1 and is 84.3% similar (48.9% identical) to GLE2. Although the four putative β-transducin/WD repeats in RAE1 and GLE2 are well conserved in SONA, the similarity between SONA and RAE1 and GLE2 extends well outside of these repeats along the entire peptide sequences (Fig. 7 *B*).

To determine the localization of SONA, we constructed strains expressing an HA epitope-tagged version of SONA (SONA-HA). SONA-HA was functional as its expression complemented the cs phenotype of *sonA1* (data not shown). Exponentially growing cells expressing SONA-HA showed punctate staining appearing as a ring at the periphery of each nucleus (Fig. 8). A no-HA control strain showed no nuclear ring staining (data not shown; also refer to Fig. 1). SONA-HA staining was not completely coincident with DAPI staining in that it was limited to the nuclear periphery and was evident at the nuclear periphery in regions next to nucleoli, where DAPI staining was excluded. The SONA-HA staining pattern was strikingly similar to the nuclear pore-like staining pattern seen for GLE2 (Murphy et al., 1996).

sonA1 Suppresses the Nuclear Division and NIME$^{Cyclin\ B}$ Localization Defects of nimA1 without Markedly Increasing NIMA or NIMX Kinase Activity

Colonies of *sonA1*, *nimA1* double mutants exhibited

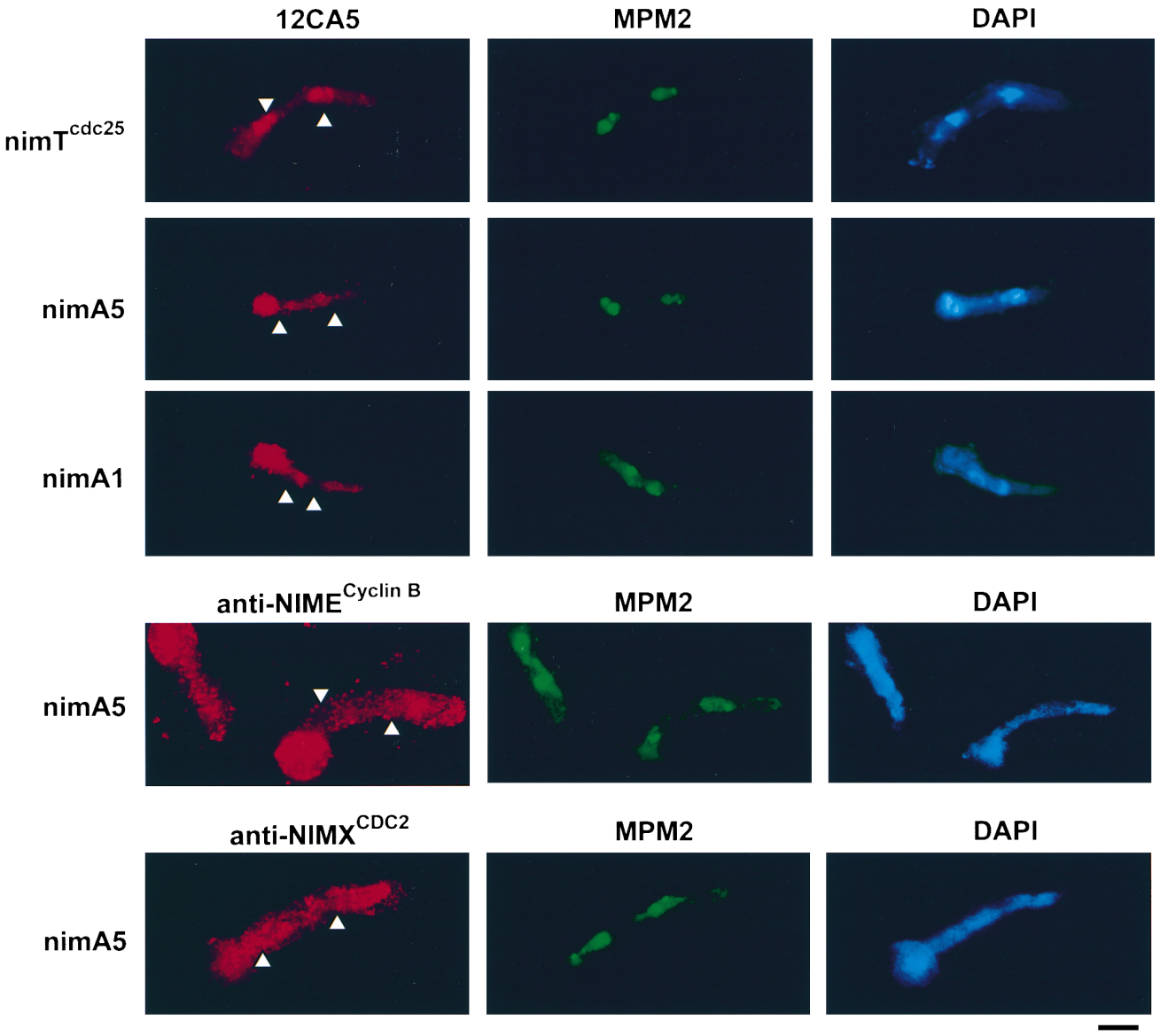

Figure 4. Nuclear-specific NIME$^{\text{Cyclin B}}$ and NIMX$^{\text{CDC2}}$ localization was prevented by *nimA* mutations. Cells of the *nimT^{cdc25}* mutant, SFC4-21, the *nimA5* mutant, PMC654-19, and the *nimA1* mutant, SFC403-19, were cultured, fixed, and then prepared for immunocytology as described in Materials and Methods. *Left*, strain identity.The images corresponding to Ab or DAPI staining are labeled at the top of the panels. *Arrows*, position of nuclei in the images showing NIME$^{\text{Cyclin B}}$ and NIMX$^{\text{CDC2}}$ localization. Bar, 10 μm.

slower growth at 42°C than either wild-type or *sonA1* single mutant strains (refer to Fig. 6). To examine the suppression of *nimA1* by *sonA1* in more detail, we followed nuclear division and nuclear morphology during spore germination in strains that were either wild-type, *nimA1*, *sonA1*, or *nimA1* plus *sonA1*. Fig. 9 shows examples of cells stained with DAPI to visualize nuclei. At 32°C (permissive growth temperature for *nimA1* and *sonA1*), essentially all of the spores from all the strains examined germinated and underwent nuclear division at approximately wild-type rates. At 42°C, the majority of *nimA1* mutant spores failed to undergo a single nuclear division even after 10 h, whereas the majority of spores from wild type had undergone 2–4 divisions. Essentially all the spores of the *nimA1*, *sonA1* double mutant germinated and underwent apparently normal nuclear divisions at 42°C. The rate of nuclear division in this strain was somewhat slower than that in wild type (data not shown). This is consistent with the reduced colony growth rate of *sonA1*, *nimA1* strains, indicating that *sonA1* does not suppress *nimA1* function to wild-type, *nimA1* levels.

It was previously shown that *nimA1* mutants arrest in G2 even though they accumulate partially active NIMA and fully activated NIMX$^{\text{CDC2}}$ (Pu et al., 1995). It was possible that *sonA1* suppresses *nimA1* by somehow increasing the level of NIMA or NIMX$^{\text{CDC2}}$ activity. To investigate these possibilities, we measured the levels of NIMA and NIMX$^{\text{CDC2}}$ kinase activities in a wild-type strain, a *nimA1*

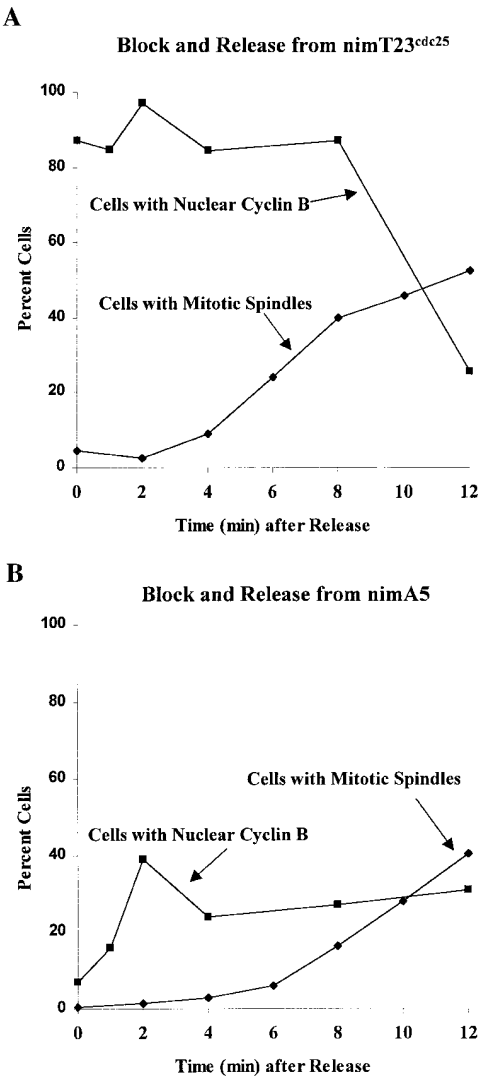

Figure 5. Cells released from the *nimA5* G2 arrest accumulate nuclear NIME$^{\text{Cyclin B}}$ before entering mitosis. Cells of the *nimT^{cdc25}* mutant, SFC4-21 (*A*), and the *nimA5* mutant, PMC654-19 (*B*), were arrested in late G2 by incubation at restrictive temperature and then released from the G2 arrest by shift to permissive temperature (refer to Materials and Methods). The cells were stained for HA-NIME$^{\text{Cyclin B}}$ to determine the percent cells with nuclear cyclin B (■) and with anti–α-tubulin to determine the percent cells with mitotic spindles (◆). Each value was determined by counting at least 100 cells.

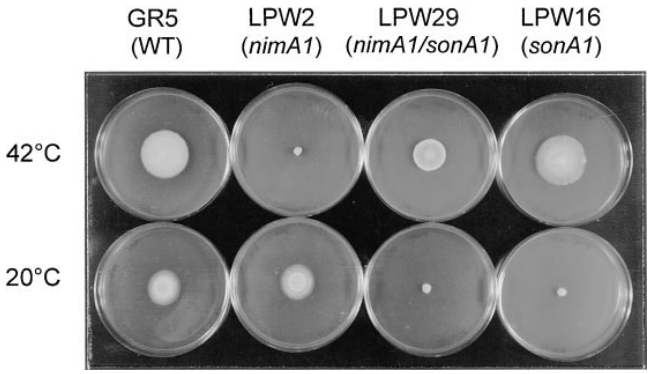

Figure 6. Colony growth phenotype of the following strains: wild-type (*GR5*), *nimA1* (*LPW2*), *sonA1* (*LPW16*), and *nimA1*, *sonA1* (*LPW29*). Strains are identified by their relevant genotype indicated at the top. Each strain was center-point inoculated on MAG medium and then incubated at 42°C for 3 d or at 20°C for 10 d, as indicated.

mutant, a *sonA1* mutant, and a *nimA1*, *sonA1* double mutant. Samples were analyzed from asynchronous cultures, from cultures shifted to restrictive temperature, and from cultures shifted to restrictive temperature and then returned to permissive temperature. Fig. 10 shows that 3 h after shift to restrictive temperature (42°C), the *nimA1* mutant, LPW2, accumulated NIMA and NIMX$^{\text{CDC2}}$ kinase to levels above that in asynchronous cultures. Return to permissive temperature induced these cells to synchronously enter mitosis, and resulted in a severalfold increase in NIMA activity but no significant increase in NIMX$^{\text{CDC2}}$ activity (Fig. 10 *C*). These results are in agreement with Pu et al. (1995), and they demonstrate that *nimA1* blocks progression into mitosis but does not prevent full activation of NIMX$^{\text{CDC2}}$. The *nimA1*, *sonA1* double mutant, LPW29, did not accumulate NIMA or NIMX$^{\text{CDC2}}$ activity above that of LPW2 either before or after a shift to 42°C (Fig. 10, *A* and *B*, compare *first* and *second panels*). Based on the peak of mitotic cells after the return to permissive temperature, ~25% of the LPW29 cells had accumulated in late G2 during incubation at 42°C, consistent with previous data showing that suppression of *nimA1* by *sonA1* is not complete. The wild-type (GR5) and *sonA1* single mutant (LPW16) were essentially identical under these conditions (Fig. 10, *A* and *B*, *third* and *fourth panels*).

Given that *sonA1* did not cause an increase in the levels of NIMA or NIMX$^{\text{CDC2}}$ activity, and that SONA is related to the GLE2/RAE1 nucelocytoplamsic transporter, we considered the possibility that *sonA1* may suppress the NIME$^{\text{Cyclin B}}$ localization defect of *nimA1* mutants. We constructed *nimA1*, *sonA1* double mutants and *nimA5*, *sonA1* double mutants which expressed HA-NIME$^{\text{Cyclin B}}$ as their only NIME$^{\text{Cyclin B}}$. Whereas *nimA1* cells cultured at restrictive temperature for *nimA1* arrested in G2 with HA-NIME$^{\text{Cyclin B}}$ staining throughout the cell, *nimA1*, *sonA1* double mutants continued to divide and showed nuclear-specific HA-NIME$^{\text{Cyclin B}}$ staining (Fig. 11). The percentage of *nimA1*, *sonA1* double mutants showing nuclear HA-NIME$^{\text{Cyclin B}}$ staining was 33% (n = 100) compared with 51% (n = 102) for wild-type cells. These results are consistent with the fact that *sonA1* only partially suppresses the growth and nuclear division phenotype of *nimA1* mutants (see Figs. 6 and 9). The *nimA5*, *sonA1* double mutant incubated at restrictive temperature arrested in G2 and did not accumulate nuclear-specific HA-NIME$^{\text{Cyclin B}}$ (data not shown), demonstrating that the ability of *sonA1* to suppress the NIME$^{\text{Cyclin B}}$ localization defect of *nimA* mutants was allele specific.

Discussion

Inactivation of the NIMA kinase causes a specific cell cycle arrest in G2 without preventing activation of the H1 kinase activity of NIMX$^{\text{CDC2}}$/NIME$^{\text{Cyclin B}}$. NIMA is, there-

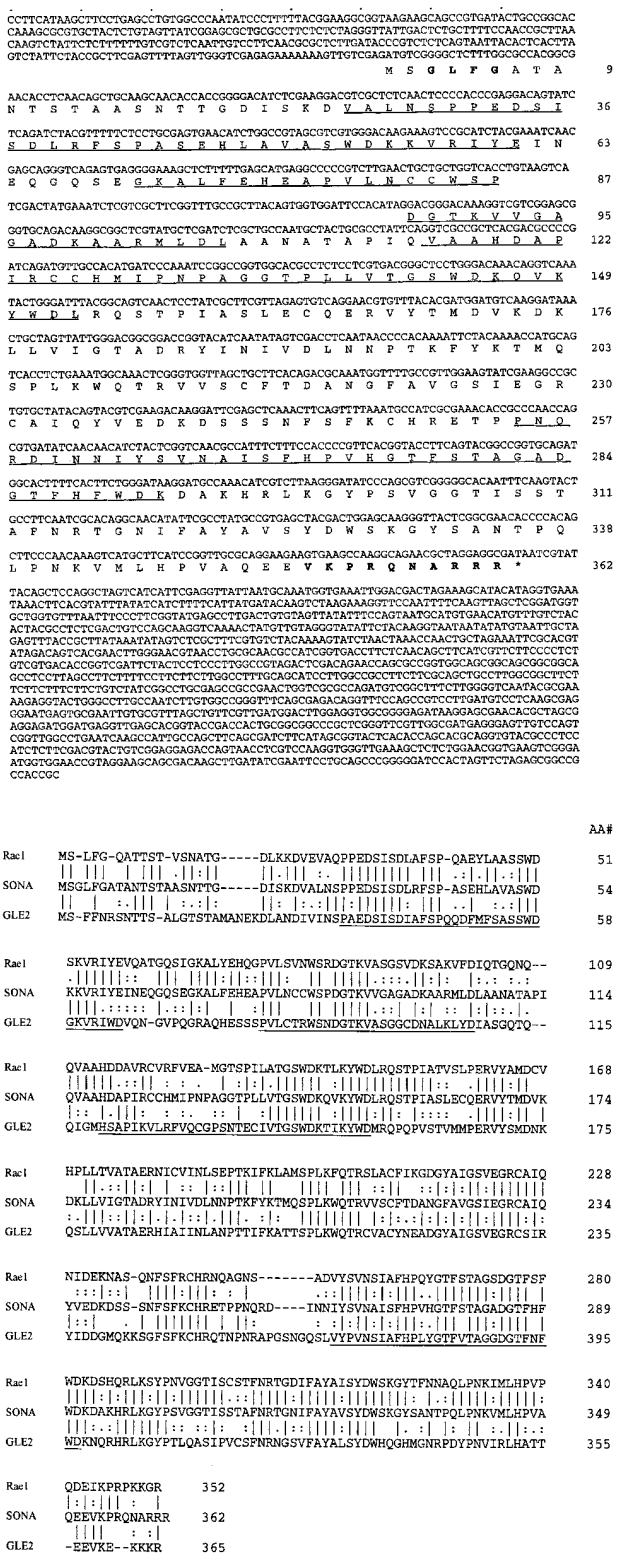

Figure 7. Sequence of *sonA* and alignment of SONA to GLE2 and RAE1. (*A*) The nucleotide sequence and predicted ORF in the 2.6-kb genomic *sonA* clone is shown. *Right*, amino acid residues of the SONA ORF; *underline*, predicted WD repeats; *boldface at the amino terminus*, a single GLFG sequence, found in multiple copies of many nuclear pore proteins; *boldface at the carboxyl terminus,* a potential nuclear localization sequence. The position of the intron was confirmed by sequencing a cDNA clone. (*B*) An alignment of SONA to GLE2 and RAE1 is shown. *Right*, amino acid residue numbers; *solid lines*, identical residues. Highly conserved and conserved residues, as determined by the Applied Biosystems Sequence Analysis Software, are indicated by the *double dots*, and *single dots*, respectively. The *sonA* cDNA sequence is available from EMBL/GenBank/DDBJ under accession number AF069492.

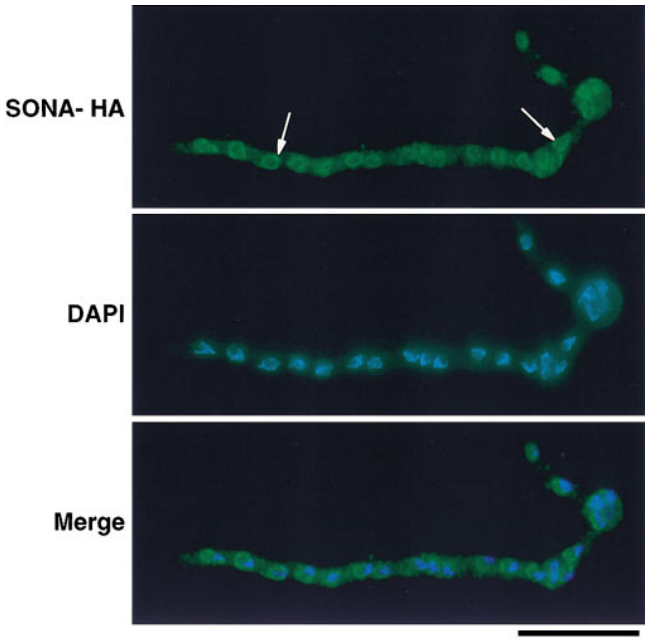

Figure 8. SONA-HA localizes to the nuclear periphery. Cells of the SONA-HA–expressing strain, LPW42, were cultured, fixed, and then prepared for immunocytology as described in Materials and Methods. The image is identified to the left (SONA-HA shows 12CA5 staining). *Arrows*, example nuclei within the multinucleate cell shown. Digital images were captured using a Sensys Photometrics CCD camera and were merged using Phase 3 Imaging Systems software. Bar, 10 μm.

fore, required for mitotic initiation by a mechanism other than activation of NIMX^{CDC2} as an H1 kinase. Although NIMA itself is probably required for normal mitosis independently of NIMX^{CDC2} (O'Connell et al., 1994; Lu and Hunter, 1995; Pu and Osmani, 1995), some mechanism must be in place to prevent activated NIMX^{CDC2} from inappropriately inducing mitosis in the absence of NIMA function. One possibility is that NIMA affects the mitosis-promoting activity of NIMX^{CDC2} at some level other than activation of enzyme activity. Two lines of evidence presented here, one genetic, the other cytological, lend support to such a hypothesis and indicate a role for NIMA in the nuclear localization of NIMX^{CDC2}/NIME$^{Cyclin\ B}$.

The NIMX^{CDC2}/NIME$^{Cyclin\ B}$ Complex Localizes to the Nucleus in a NIMA-dependent Manner

We have shown that the major *A. nidulans* B-type cyclin, NIME$^{Cyclin\ B}$, localized to the chromatin, nucleolar, and SPB regions of the nucleus in a NIMA-dependent manner. NIME$^{Cyclin\ B}$ localization to the nucleus in S and G2 parallels its accumulation (Ye et al., 1995, 1996), similar in many respects to localization of the *S. pombe* G2 cyclin, p63^{cdc13} (Booher et al., 1989; Alfa et al., 1990, 1991; Gal-

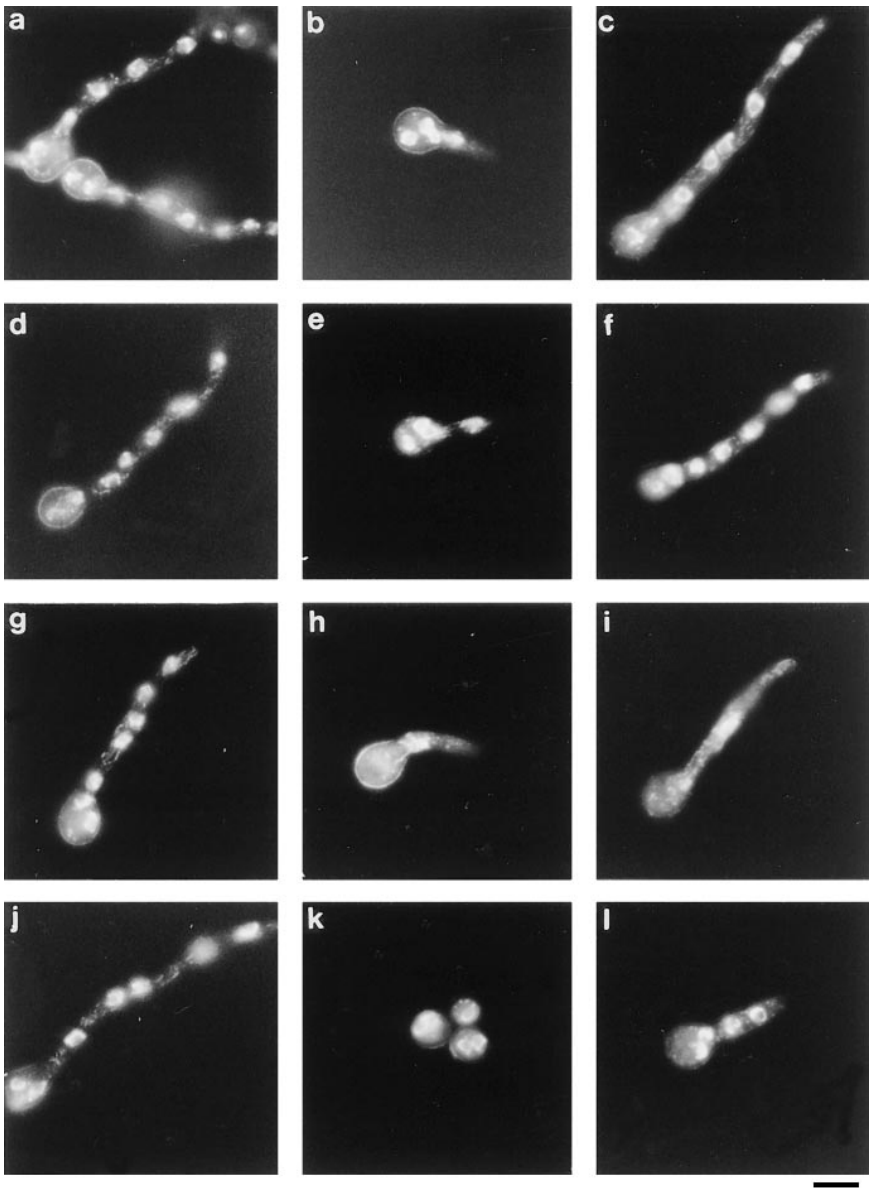

Figure 9. Nuclear division in wild-type–, *nimA1*-, and *sonA1*-containing strains. Cells of the wild-type strain, GR5 (*a–c*), the *sonA1* mutant, LPW16 (*d–f*), the *nimA1* mutant, LPW2 (*g–i*), and the *nimA1*, *sonA1* double mutant, LPW19 (*j–l*) were stained with DAPI as described in Materials and Methods. Cells shown in panels *a, d, g,* and *j* were incubated at 32°C for 8 h. Other panels show cells incubated at 42°C for 8 h (*b, e, h,* and *k*) or 10 h (*c, f, i,* and *l*). Bar, 10 μm.

lagher et al., 1993; however, also see Audit et al., 1996 for evidence of cytoplasmic p63^{cdc13} localization during interphase). The localization of NIMX^{CDC2} to the nucleus correlated with that of NIME$^{Cyclin\ B}$ and was also dependent on NIMA function, suggesting that localization of NIMX^{CDC2}/NIME$^{Cyclin\ B}$ complex itself is perturbed in *nimA* mutants.

We noted no obvious nuclear NIME$^{Cyclin\ B}$ staining in metaphase cells, even though we have looked at well over a thousand cells from cultures synchronously entering mitosis. We did observe nuclear staining very early in mitosis, before significant SPB separation. These results differ somewhat from cyclin B localization to the mitotic apparatus at metaphase in *S. pombe* and mammalian cells (for examples see Alfa et al., 1990; Pines and Hunter, 1991; Gallant and Nigg, 1992; Jackman et al., 1995), however, the significance of this difference is not clear. Either we cannot detect whatever NIME$^{Cyclin\ B}$ is present in metaphase nuclei or NIME$^{Cyclin\ B}$ is lost from the nucleus before metaphase. We are currently investigating NIME$^{Cyclin\ B}$ localization in cells overexpressing NIME$^{Cyclin\ B}$ and in cells blocked in mitosis by drugs or by cell cycle mutations to clarify this issue.

NIMA and SONA in the Nucleocytoplasmic Transport of NIME$^{Cyclin\ B}$

The mechanism by which NIMA functions to promote nuclear NIME$^{Cyclin\ B}$ localization may be indicated by the identification of *sonA* as an allele-specific suppressor of *nimA1*. SONA shows high sequence similarity to RAE1 of *S. pombe* (Brown et al., 1995), GLE2 of *S. cerevisiae* (Murphy et al., 1996), and the mammalian protein, MRNP41 (Kraemer and Blobel, 1997), all of which have been implicated in nucleocytoplasmic transport. The nuclear mRNA export defect in *rae1*$^-$and *gle2*$^-$mutants, and the association of MRNP41 with mRNA indicate an important role for these proteins in mRNA export. However, none of

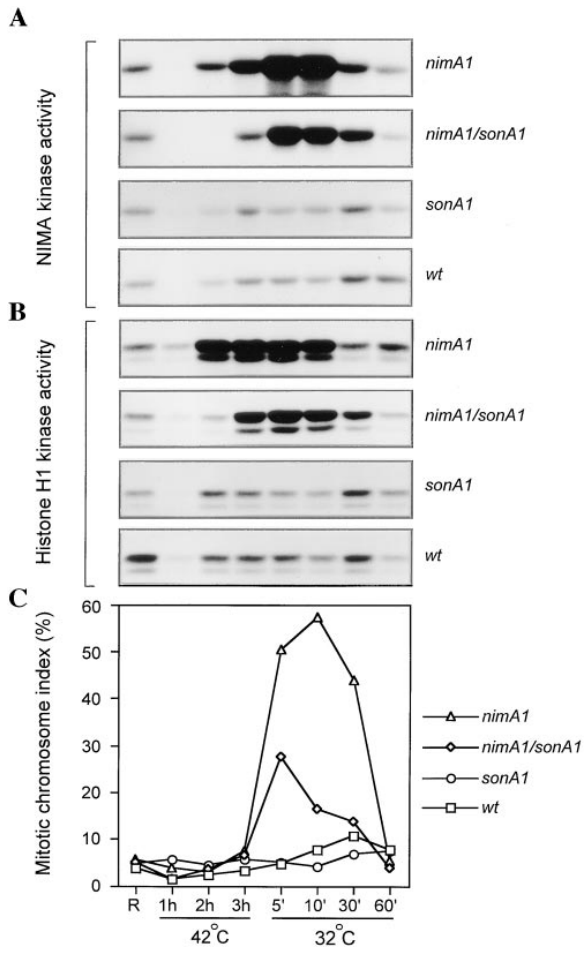

Figure 10. NIMA and NIMX^{CDC2} kinase activities in wild-type–, *nimA1*-, and *sonA1*-containing strains. Cells of a wild-type strain (GR5), a *nimA1* containing strain (LPW2), a *sonA1*-containing strain (LPW16), and a *nimA1*, *sonA1* double mutant strain (LPW29) were cultured and then sampled for kinase activity (A and *B*) and percentage of mitotic cells (*C*) as described in Materials and Methods. Samples were taken from exponentially growing, asynchronous cultures (*R*) or from cultures shifted to 42°C for 1, 2, or 3 h, or from cultures returned to 32°C for 5, 10, 30, or 60 min. *A* and *B* show autoradiographs representing NIMA (*A*) and NIMX^{CDC2} (*B*) kinase activities measured in immune complexes isolated from whole cell extracts from the strains indicated at the right.

these proteins contain RNA binding motifs, suggesting that their interaction with mRNA is indirect. Furthermore, GLE2 and MRNP41 localize predominantly to nuclear pore complexes, *gle2*$^-$ mutations derange nuclear pore complex structure, and GLE2 interacts with SRP1 (importin α) in a two-hybrid assay, suggesting that these proteins play a more general role in nucleocytoplasmic transport (Murphy et al., 1996; Kraemer and Blobel, 1997). The localization of SONA to the nuclear periphery (refer to Fig. 8) is consistent with a role for SONA in nucleocytoplasmic transport.

Given that proper NIME$^{Cyclin\ B}$ localization is dependent on NIMA function (refer to Fig, 4), and that the *sonA1* mutation suppresses the mitotic and NIME$^{Cyclin\ B}$ localization defect in *nimA1* mutants without causing an increase in NIMA or NIMX^{CDC2} activity (refer to Fig. 10), we propose that NIMA and SONA are involved in the nucleocytoplasmic transport of NIME$^{Cyclin\ B}$. Two models consistent with our results (Fig. 12) propose that nuclear localization of NIME$^{Cyclin\ B}$ is a function of its rate of import into the nucleus and its rate of export into the cytoplasm (Fig. 12). These models predict that localization of NIME$^{Cyclin\ B}$ to the SPB is dependent on its accumulation in the nucleus, as if NIME$^{Cyclin\ B}$ accumulates at the nucleoplasmic surface of the SPB. This prediction is consistent with the fact that the SPB is tightly associated with the nucleus throughout the cell cycle in *A. nidulans* (Oakley and Morris, 1983). SONA is proposed to play a positive role in nuclear export, based on the mRNA export defects of *rae1*/*gle2* mutants, although we cannot formerly exclude a role for SONA in nuclear import. NIMA is proposed to oppose SONA function, either by facilitating nuclear import (Fig. 12 *A*), or by antagonizing export (Fig. 12 *B*). In either scenario, loss of NIMA function results in a net decrease in nuclear NIME$^{Cyclin\ B}$, which can be offset by loss of SONA function.

These models are not meant to exclude additional functions for NIMA beyond that in the nucleocytoplasmic transport of NIMX^{CDC2}/NIME$^{Cyclin\ B}$. The finding that gain of function mutations in *nimA* can induce abnormal mitosis in the absence of CDC2 function (O'Connell et al., 1994; Lu and Hunter, 1995; Pu and Osmani, 1995) clearly indicates that NIMA has additional roles in promoting mitosis.

We have proposed a specific (although not necessarily physical) interaction between NIMA and SONA in controlling nuclear NIME$^{Cyclin\ B}$ levels because of the allele-specific suppression of *nimA1* (and not *nimA5*) by *sonA1*. The mechanism underlying this allele-specific interaction may be explained by quantitative differences in NIMA kinase activity in *nimA1* versus *nimA5* mutants. For example, extracts from cells arrested in G2 by the *nimA1* mutation contain residual NIMA kinase activity (refer to Fig 10; Pu et al., 1995), whereas equivalent extracts from *nimA5* cells contain only trace NIMA kinase levels (Ye et al., 1995). Accordingly, the *nimA5* mutation may cause too severe a defect in the nuclear accumulation of NIME$^{Cyclin\ B}$ for the *sonA1* mutation to suppress. Alternatively, the allele-specific *nimA1*/*sonA1* interaction may be due to a direct interaction between NIMA and SONA. In this regard, we note that SONA contains three consensus NIMA phosphorylation sites (Lu et al., 1994) (refer to Fig. 7; FGAT at 5–8, FYKT at 198–201, and FNRT at 31–316). Regardless of the underlying mechanism, the allele-specific interaction between *nimA* and *sonA* indicates a specific interaction and demonstrates that inactivation of *sonA* does not simply bypass the need for *nimA* in the promotion of mitosis.

Nucleocytoplasmic Transport and Regulation of Mitosis

This study establishes a role for NIMA in the nuclear localization of NIMX^{CDC2}/NIME$^{Cyclin\ B}$. One implication of this finding is that nucleocytoplasmic transport and regulation of mitosis are intimately linked. Such transport is particularly relevant to closed mitosis, in which the nuclear envelope remains intact, as occurs in many fungi including *A. nidulans*, *S. pombe*, and *S. cerevisiae*. At the very least,

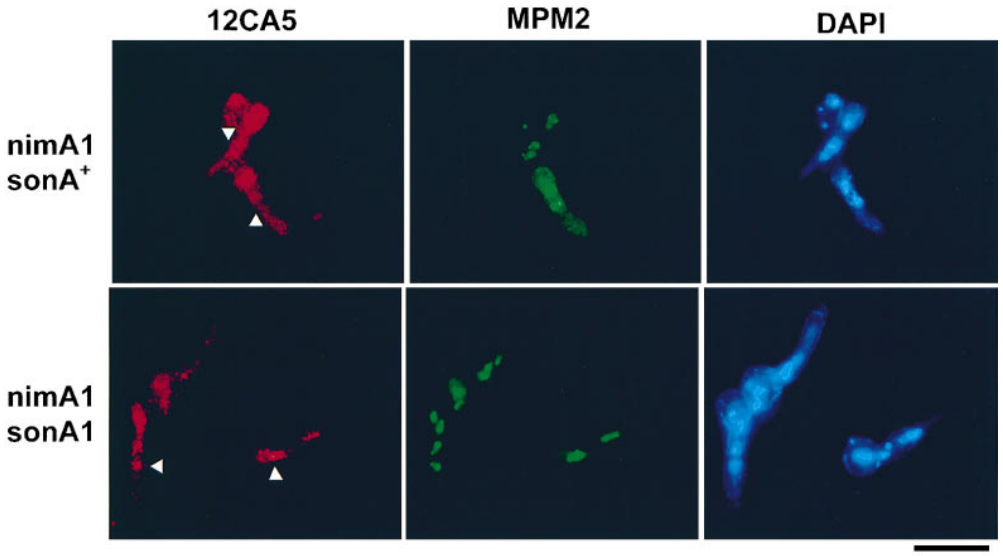

Figure 11. The *sonA1* mutation suppresses the nuclear NIME$^{\text{Cyclin B}}$ localization defect of *nimA1*. Cells of the *nimA1* strain, SFC403-19, and the *nimA1*, *sonA1* double mutant, SFC444-1, were cultured, fixed, and then prepared for immunocytology as described in Materials and Methods. *Left*, strain identity; *top*, images corresponding to Ab or DAPI staining; *top row arrows*, (*nimA1* single mutant) position of nuclei in cells showing general cytoplasmic staining; *bottom row arrows,* position of example nuclei showing NIME$^{\text{Cyclin B}}$ staining. Bar, 10 μm.

tubulin from disintegrated cytoplasmic microtubules probably needs to be rapidly imported into nuclei to form the intranuclear spindle. Regulators of mitosis may also undergo nuclear or cytoplasmic transport at mitosis, as was proposed for the p107$^{\text{wee1}}$ regulator, p70$^{\text{nim1}}$ in *S. pombe* (Wu and Russell, 1997). A causal relationship between transport and mitosis is also supported by the G2/M arrest due to a mutation in the *S. cerevisiae SRP1* (importin α) gene (Loeb et al., 1995) and by the finding that the *S. pombe rae1*$^{-}$ mutation causes a G2 arrest (Brown et al., 1995).

Another significant implication of this work is the identification of a mechanism by which NIMX$^{\text{CDC2}}$/NIME$^{\text{Cyclin B}}$ function is coordinated with that of NIMA. The requirement for the function of both kinases for the initiation of mitosis can now be explained by a model in which each kinase independently promotes some events of mitosis while also being sensitive to the function of the other. In this model, NIMA is not fully functional until it is hyperphosphorylated by NIMX$^{\text{CDC2}}$/NIME$^{\text{Cyclin B}}$ and NIMX$^{\text{CDC2}}$/NIME$^{\text{Cyclin B}}$ is not properly localized unless NIMA is functional. Given the finding of NIMA-like functions in other organisms (O'Connell et al., 1994; Fry and Nigg, 1995; Gallant et al., 1995; Pu et al., 1995; Pu and Osmani, 1995; Lu and Hunter, 1995), and the evolutionary conservation of SONA/GLE2/RAE1/MNRP41 (refer to Fig. 7; Brown et al., 1995; Murphy et al., 1996; Kraemer and Blobel, 1997), the analysis of NIMA and SONA interactions in *A. nidulans* should serve as an important model for the elucidation of fundamental mechanisms coordinating nucleocytoplasmic transport and mitosis.

Finally, it is very interesting that mutation of *rae1* of *S. pombe* results in a G2 arrest without preventing full activation of p34$^{\text{cdc2}}$ (Brown et al., 1995; Whalen et al., 1997). Perhaps mutation of *rae1* prevents correct localization of p34$^{\text{cdc2}}$/p63$^{\text{cdc13}}$, which would further indicate the conserved nature of this level of mitotic regulation.

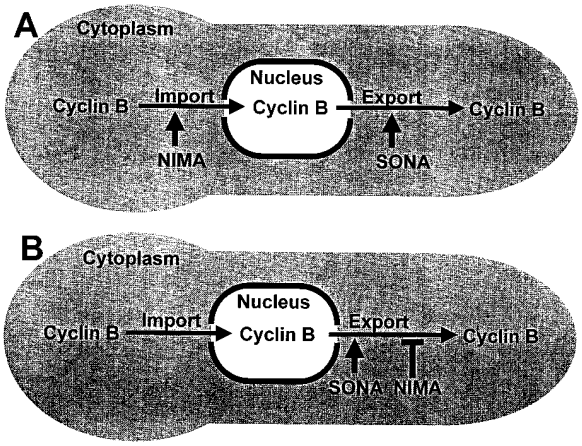

Figure 12. Model for NIMA and SONA function in the nucleocytoplasmic transport of NIME$^{\text{Cyclin B}}$.

P.M. Mirabito thanks D.A. Harrison (University of Kentucky, Lexington, KY) for use of his image station and for his skill and patience in helping with imaging and figure preparation. The authors also thank members of the Mirabito and Osmani laboratories, particularly S. Venkatram, for helpful discussions throughout this work and for critical reading of the manuscript.

This work was supported by NIH grants to P.M. Mirabito (GM51931) and S.A.Osmani (GM42564).

Received for publication 10 September 1997 and in revised form 8 May 1998.

References

Alfa, C.E., B. Ducommun, D. Beach, and J.S. Hyams. 1990. Distinct nuclear and spindle pole body populations of cyclin*cdc2* in fission yeast. *Nature.* 347: 680–682.

Alfa, C.E., I.M. Gallagher, and J.S. Hyams. 1991. Subcellular localization of the p34$^{\text{cdc2}}$/p63$^{\text{cdc13}}$ protein kinase in fission yeast. *Cold Spring Harbor Symp. Quant. Biol.* 56:489–494.

Altschul, S.F., W. Gish, W. Miller, E.W. Myers, and D.J. Lipman. 1990. Basic local alignment search tool. *J. Mol. Biol.* 215:403–410.

Audit, M., M. Barbier, M.O. Soyer-Gobillard, M. Albert, M.L. Geraud, G. Nicolas, and G. Lenaers. 1996. Cyclin B (p56$^{\text{cdc13}}$) localization in the yeast *Schizosaccharomyces pombe*: an ultrastructural and immunocytochemical study. *Biol. Cell.* 86:1–10.

Bergen, L.G., A. Upshall, and N.R. Morris. 1984. S phase, G2 and nuclear division mutants of *Aspergillus nidulans*. *J. Bact.* 159:114–119.

Booher, R.N., C.E. Alfa, J.H. Hyams, and D.H. Beach. 1989. The fission yeast *cdc2/cdc13/suc1* protein kinase: regulation of catalytic activity and nuclear localization. *Cell.* 58:485–497.

Brody, H., J. Griffith, A.J. Cuticchia, J. Arnold, and W.E. Timberlake. 1991. Chromosome specific recombinant DNA libraries from the fungus *Aspergillus nidulans*. *Nucl. Acids Res.* 19: 3105–3109.

Brown, J.A., A. Bharathi, A. Ghosh, W. Whalen, E. Fitzgerald, and R. Dhar. 1995. A mutation in the *Schizosaccharomyces pombe rae1* gene causes defects in poly(A)1 RNA export and in the cytoskeleton. *J. Biol. Chem.* 270: 7411–7419.

Fry, A.M., and E.A. Nigg. 1995. Cell cycle. The NIMA kinase joins forces with Cdc2. *Curr. Biol*. 5:1122–1125.

Gallagher, I.M., C.E. Alfa, and J.S. Hyams. 1993. $p63^{cdc13}$, a B type cyclin, is associated with both the nucleolar and chromatin domains of the fission yeast nucleus. *Mol. Biol. Cell.* 4:1087–1096.

Gallant, P., and E.A. Nigg, 1992. Cyclin B2 undergoes cell cycle dependent nuclear translocation and, when expressed as a nondestructible mutant, causes mitotic arrest in HeLa cells. *J. Cell Biol.* 117:213–224.

Gallant, P., A.M. Fry, and E.A. Nigg. 1995. Protein kinases in the control of mitosis: focus on nucleocytoplasmic trafficking. *J. Cell Sci.* 19(Suppl.):21–28.

Gems, D., I.L. Johnstone, and J.C. Clutterbuck. 1991. An autonomously replicating plasmid transforms *Aspergillus nidulans* at high frequency. *Gene.* 98: 61–67.

Gems, D., A. Aleksenko, L. Belenky, S. Robertson, M. Ramsden,Y. Vinetski, and A.J. Clutterbuck. 1994. An "instant gene bank" method for gene cloning by mutant complementation. *Mol. Gen. Genet.* 242:467–471.

Harris, S.D., J.L. Morrell, and J.E. Hamer. 1994. Identification and characterization of *Aspergillus nidulans* mutants defective in cytokinesis. *Genetics.* 136: 517–532.

Jackman, M., M. Firth, and J. Pines. 1995. Human cyclins B1 and B2 are localized to strikingly different structures: B1 to microtubules, B2 primarily to the Golgi apparatus. *EMBO (Eur. Mol. Biol. Organ.) J.* 14:1646–1654.

James, S.W., P.M. Mirabito, P.C. Scacheri, and N.R. Morris. 1995. The *Aspergillus nidulans bimE* (blocked in mitosis) gene encodes multiple cell cycle functions involved in mitotic checkpoint control and mitosis. *J. Cell Sci.* 108: 3485–3499.

Kafer, E. 1977. Meiotic and mitotic recombination in *Aspergillus nidulans* and its chromosomal aberrations. *Adv. Genet.* 19:33–131.

Kraemer, D., and G. Blobel. 1997. mRNA binding protein mrnp 41 localizes to both nucleus and cytoplasm. *Proc. Natl. Acad. Sci. USA*. 94:9119–9124.

Loeb, J.D., G. Schlenstedt, D. Pellman, D. Kornitzer, P.A. Silver, and G.R. Fink. 1995. The yeast nuclear import receptor is required for mitosis. *Proc. Natl. Acad. Sci. USA*. 92:7647–7651.

Lu, K.P., S.A. Osmani, and A.R. Means. 1993. Properties and regulation of the cell cycle-specific NimA protein kinase of *Aspergillus nidulans*. *J. Biol. Chem.* 268:8769–8776.

Lu, K.P., B.E. Kemp, and A.R. Means. 1994. Identification of substrate specificity determinants for the cell cycle regulated NIMA protein kinase. *J. Biol. Chem.* 269:6603–6607.

Maridor, G, P. Gallant, R. Golsteyn, and E.A. Nigg. 1993. Nuclear localization of vertebrate cyclin A correlates with its ability to form complexes with cdk catalytic subunits. *J. Cell Sci.* 106:535–544.

Martin, M.A., S.A. Osmani, and B.R. Oakley. 1997. The role of gtubulin in mitotic spindle formation and cell cycle progression in *Aspergillus nidulans*. *J. Cell Sci.* 110:623–633.

Mirabito, P.M., and N.R. Morris. 1993. BIMA, a TPR-containing protein required for mitosis, localizes to the spindle pole body in *Aspergillus nidulans*. *J. Cell Biol.* 120:959–968.

Morris, N.R. 1976. Mitotic mutants of *Aspergillus nidulans*. *Genet. Res.* 26: 237–254.

Murphy, R., J.L. Watkins, and S.R. Wente. 1996. GLE2, a *Saccharomyces cerevisiae* homologue of the *Schizosaccharomyces pombe* export factor RAE1, is required for nuclear pore complex structure and function. *Mol. Biol. Cell.* 7:1921–1937.

Nurse, P. 1990. Universal control mechanism regulating onset of M phase. *Nature.* 344:503–508.

Oakley, B.R., and N.R. Morris. 1983. A mutation in *Aspergillus nidulans* that blocks the transition from interphase to prophase. *J. Cell Biol.* 96:1155–1158.

O'Connell, M.J., A.H. Osmani, N.R. Morris, and S.A. Osmani. 1992. An extra copy of $nimE^{cyclinB}$ elevates pre-MPF levels and partially suppresses mutation of $nimT^{cdc25}$ in *Aspergillus nidulans*. *EMBO (Eur. Mol. Biol. Organ.) J.* 11:2139–2149.

O'Connell, M.J., C. Norbury, and P. Nurse. 1994. Premature chromatin condensation upon accumulation of NIMA. *EMBO (Eur. Mol. Biol. Organ.) J.* 13: 4926–4937.

Ookata, K., S. Hisanaga, T. Okano, K. Tachibana, and T. Kishimoto. 1992. Relocation and distinct subcellular localization of $p34^{cdc2}$-cyclin B at meiosis reinitiation in starfish oocytes. *EMBO (Eur. Mol. Biol. Organ) J.* 11:1763–1772.

Ookata, K, S. Hisanaga, J.C. Bulinski, H. Murofushi, H. Aizawa, T.J. Itoh, H. Hotani, E. Okumura, K. Tachibana, and T. Kishimoto. 1995. Cyclin B interaction with microtubule-associated protein 4 (MAP4) targets $p34^{cdc2}$ kinase to microtubules and is a potential regulator of M-phase microtubule dynamics. *J. Cell Biol.* 128:849–862.

Osmani, S.A., G.S. May, and N.R. Morris. 1987. Regulation of the mRNA levels of *nimA*, a gene required for the G2M transition in *Aspergillus nidulans*. *J. Cell Biol.* 104:1495–1504.

Osmani, S.A., D.B. Engle, J.H. Doonan, and N.R. Morris. 1988*a*. Spindle formation and chromatin condensation in cells blocked at interphase by mutation of a negative cell cycle control gene. *Cell.* 52:241–251.

Osmani, S.A., R.T. Pu, and N.R. Morris. 1988*b*. Mitotic induction and maintenance by overexpression of a G2specific gene that encodes a potential protein kinase. *Cell.* 53:237–244.

Osmani, A., S.L. McGuire, and S.A. Osmani. 1991*a*. Parallel activation of the NIMA and $p34^{cdc2}$ cell cycle-regulated protein kinases is required to initiate mitosis in *A. nidulans*. *Cell.* 67: 283–291.

Osmani, A.H., K. O'Donnell, R.T. Pu, and S.A. Osmani. 1991*b*. Activation of the *nim*A protein kinase plays a unique role during mitosis that cannot be bypassed by absence of the *bim*E checkpoint. *EMBO (Eur. Mol. Biol. Organ.) J.* 10:2669–2679.

Osmani, A.H., N. van Peij, M. Mischke, M.J. O'Connell, and S.A. Osmani. 1994. A single $p34^{cdc2}$ protein kinase (encoded by $nimX^{cdc2}$) is required at G_1 and G_2 in *Aspergillus nidulans*. *J. Cell Sci.* 107:1519–1528.

Pines, J., and T. Hunter. 1991. Human cyclins A and B1 are differentially located in the cell and undergo cell cycle-dependent nuclear transport. *J. Cell Biol.* 115:1–17.

Pontecorvo, G., J.A. Roper, L.M. Hemmons, K.D. MacDonald, and A.W.J. Buffon. 1953. The genetics of *Aspergillus nidulans*. *Adv. Genet.* 5:141–238.

Pu, R.T., and S.A Osmani. 1995. Mitotic destruction of the cell cycle regulated NIMA protein kinase of *Aspergillus nidulans* is required for mitotic exit. *EMBO (Eur. Mol. Biol. Organ.) J.* 14:995–1003.

Pu, R.T., G. Xu, L. Wu, J. Vierula, K. O'Donnell, X.S. Ye, and S.A.Osmani. 1995. Isolation of a functional homolog of the cell cycle specific NIMA protein kinase of *Aspergillus nidulans* and functional analysis of conserved residues. *J. Biol. Chem.* 270:18110–18116.

Sambrook, J., E.F. Fritsch, and T. Maniatis. 1989. Molecular Cloning: A Laboratory Manual. Cold Spring Harbor Laboratory Press, Cold Spring Harbor, NY. 545 pp.

Verdoes, J.C., P.J. Punt, P. van der Berg, F. Debets, A.H. Stouthamer, and C.A.M. van den Hondel. 1994. Characterization of an efficient gene cloning strategy for *Aspergillus niger* based on an autonomously replicating plasmid: cloning of the nicB gene of *A. niger. Gene*. 146:159–165.

Waring, R.B., G.S. May, and N.R. Morris. 1989. Characterization of an inducible expression system in *Aspergillus nidulans* using alcA and tubulin coding genes. *Gene.* 79:119–130.

Whalen, W.A., A. Bharathi, D. Danielewicz, R. Dhar. 1997. Advancement through mitosis requires *rae1* gene function in fission yeast. *Yeast.* 13:1167–1179.

Wu, L., and P. Russell. 1997. Nif1, a novel mitotic inhibitor in *Schizosaccharomyces pombe*. *EMBO (Eur Mol. Biol. Organ.) J.* 16:1342–1350.

Ye, X.S., G. Xu, R.T. Pu, R.R. Fincher, S.L. McGuire, A.H. Osmani, and S.A.Osmani. 1995. The NIMA protein kinase is hyperphosphorylated and activated downstream of $p34^{cdc2}$/cyclin B: Coordination of two mitosis promoting kinases. *EMBO (Eur. Mol. Biol. Organ.) J.* 14:986–994.

Ye, X.S., R.R. Fincher, A. Tang, K. O'Donnell, and S.A. Osmani. 1996. Two S phase checkpoint systems, one involving the function of both BIME and Tyr15 phosphorylation of $p34^{cdc2}$, inhibit NIMA and prevent premature mitosis. *EMBO (Eur. Mol. Biol. Organ.) J.* 1996. 15: 3599–3610.